

## ARCHITECTURE OF PLANETARY SYSTEMS BASED ON *KEPLER* DATA: NUMBER OF PLANETS AND COPLANARITY

JULIA FANG<sup>1</sup> AND JEAN-LUC MARGOT<sup>1,2</sup>

<sup>1</sup> Department of Physics and Astronomy, University of California, Los Angeles, CA 90095, USA

<sup>2</sup> Department of Earth and Space Sciences, University of California, Los Angeles, CA 90095, USA  
Received 2012 July 22; accepted 2012 October 30; published 2012 November 28

### ABSTRACT

We investigated the underlying architecture of planetary systems by deriving the distribution of planet multiplicity (number of planets) and the distribution of orbital inclinations based on the sample of planet candidates discovered by the *Kepler* mission. The scope of our study included solar-like stars and planets with orbital periods less than 200 days and with radii between 1.5 and 30 Earth radii, and was based on *Kepler* planet candidates detected during Quarters 1–6. We created models of planetary systems with different distributions of planet multiplicity and inclinations, simulated observations of these systems by *Kepler*, and compared the properties of the transits of detectable objects to actual *Kepler* planet detections. Specifically, we compared with both the *Kepler* sample’s transit numbers and normalized transit duration ratios in order to determine each model’s goodness of fit. We did not include any constraints from radial velocity surveys. Based on our best-fit models, 75%–80% of planetary systems have one or two planets with orbital periods less than 200 days. In addition, over 85% of planets have orbital inclinations less than 3° (relative to a common reference plane). This high degree of coplanarity is comparable to that seen in our solar system. These results have implications for planet formation and evolution theories. Low inclinations are consistent with planets forming in a protoplanetary disk, followed by evolution without significant and lasting perturbations from other bodies capable of increasing inclinations.

*Key words:* methods: statistical – planetary systems – planets and satellites: detection – planets and satellites: general

*Online-only material:* color figures

### 1. INTRODUCTION

Knowledge of the architecture of planetary systems can provide important constraints and insights into theories of planet formation and evolution. For instance, planetary systems with a high degree of coplanarity or alignment, such as the solar system, are consistent with the standard formation model of planets forming in a protoplanetary disk. Additionally, planetary systems with inclined or misaligned orbits can be indicative of past events that increased eccentricities and inclinations (e.g., Kozai oscillations by outlying perturbers, resonant encounters between planets, or planet–planet scattering). Consequently, information on planetary multiplicity and the distribution of inclinations can reveal fundamental events in the lives of planetary systems as well as test theories of planet formation and evolution.

Because of observational biases, it may be difficult to reliably assess the underlying multiplicity of planets and their inclination distributions. Planets may go undetected if they have masses/radii below detection limits or if they are non-transiting (for the case of transit surveys). As for inclinations, mutual (or relative) inclinations between planets in the same system have only been measured in a limited number of cases or indirectly constrained. Examples include the planets orbiting the pulsar PSR B1257+12 (Konacki & Wolszczan 2003), the planets GJ 876 b and c using radial velocity and/or astrometric data (Bean & Seifahrt 2009; Correia et al. 2010; Baluev 2011), *v* And planets c and d using astrometric and radial velocity data (McArthur et al. 2010), using transit timing/duration analyses to constrain inclinations in the Kepler-9 system (Holman et al. 2010), Kepler-10 system (Batalha et al. 2011; Fressin et al. 2011), and Kepler-11 system

(Lissauer et al. 2011a), and analyzing transits of planets over starspots for Kepler-30 (Sanchis-Ojeda et al. 2012).

However, there now exists substantial knowledge about a large sample of planetary systems that can be used to statistically determine the underlying number of planets in each system and their relative orbital inclinations. In particular, the haul of planetary candidates cataloged by the *Kepler* mission (current count is over 2300; Borucki et al. 2011a, 2011b; Batalha et al. 2012) provides a large trove of systems to study. These *Kepler* detections are termed planetary candidates because most of them have not been formally confirmed as real planets by independent observations such as radial velocity detections or successful elimination of false positive scenarios. We will refer to *Kepler* planetary candidates interchangeably as planetary “candidates” or “planets.”

In the present study, we use the latest *Kepler* catalog of planetary candidates (identified in Quarters 1–6) released by Batalha et al. (2012) to constrain the underlying multiplicity and inclinations of planetary systems discovered by *Kepler*. By “underlying,” we are referring to our estimate of the true distributions free of observational biases. In our analysis, we create thousands of model populations, each obeying different underlying multiplicity and inclination distributions. These planetary systems are subject to artificial observations to determine which planets could be transiting and detectable by *Kepler*. The detectable planets and their properties are compared to the observed sample to determine each model’s goodness of fit to the data. Our results show that the underlying architecture of planetary systems is typically thin (low relative inclinations) with few planets with orbital periods under 200 days. Similarly, other statistical studies have been performed to constrain multiplicity and/or

inclinations using different methodologies or data sets (e.g., Lissauer et al. 2011b; Tremaine & Dong 2012; Figueira et al. 2012; Fabrycky et al. 2012; Weissbein et al. 2012; Johansen et al. 2012). Our analysis improves on previous work by including all available *Kepler* quarters, extending to 200 day orbital periods, and fitting models to observables such as normalized transit duration ratios that contain information on mutual orbital inclinations; these improvements lead to a deeper investigation of the intrinsic distributions of planetary systems.

This paper is organized as follows. Section 2 provides details on how we created model populations including choice of stellar and planetary properties. Section 3 describes how we determined detectable, transiting planets from our simulated populations as well as our methods for determining each model’s goodness of fit compared to observations. Section 4 presents our main results with analysis of our best-fit models. Section 5 includes comparisons of our results with the solar system and with previous work. Lastly, Section 6 summarizes the main conclusions of our study.

## 2. CREATING MODEL POPULATIONS

This section describes our methods for creating model populations. Each model population consists of approximately  $10^6$  simulated planetary systems from which we determine planets detectable by *Kepler*. In total, we created thousands of model populations obeying different underlying planet (1) multiplicity and (2) inclination distributions.

### 2.1. Stellar Properties

Each model population’s planetary systems have host stars with parameters drawn from a distribution of stellar properties. For each simulated system, we randomly drew a star from a subset of the quarterly *Kepler* Input Catalog (KIC; Brown et al. 2011) Combined Differential Photometric Precision (CDPP) lists<sup>3</sup> (Christiansen et al. 2012). There is a separate list per quarter because each file only lists targets observed that quarter and their corresponding CDPP noise levels over 3, 6, and 12 hr. These quarterly lists also include basic KIC parameters (unchanging in the quarterly lists) for each observed star such as its *Kepler* magnitude  $K_p$ , effective temperature  $T_{\text{eff}}$ , surface gravity parameter  $\log(g)$ , and radius  $R_*$ .

We created a subset of the KIC CDPP lists in the following manner. First, we collected the KIC CDPP lists for Quarters 1–6 (Q1–6). Not all stars are observed each quarter and we counted a total of 189,998 unique stars observed at some point during Q1–6. Next, we filtered this list of unique stars such that we only included stars that were observed under the “exoplanet” program, have nonzero values for  $R_*$  and CDPP entries, and obey the following restrictions:

$$\begin{aligned} 4100 \text{ K} &\leq T_{\text{eff}} \leq 6100 \text{ K}, \\ 4.0 &\leq \log(g \text{ [cm s}^{-2}\text{)}) \leq 4.9, \\ K_p &\leq 15 \text{ mag.} \end{aligned} \quad (1)$$

These stellar cuts allowed us to consider the brighter main-sequence stars with well-characterized properties in the KIC (consistent with those in Howard et al. 2012). With such filtering, we were left with a KIC subset of 59,224 remaining unique stars, which is roughly one-third of the original list of unique stars. For each star in this KIC subset, we calculated median CDPP values over 3, 6, and 12 hr from all the values available in the Q1–6

lists. We also used each star’s surface gravity parameter  $\log(g)$  and  $R_*$  values, which are common across the Q1–6 KIC CDPP lists, to calculate each star’s mass. Finally, we recorded each star’s observing history over Q1–6 as indicated by the quarterly KIC CDPP lists.

Our subset of the KIC with 59,224 stars was the catalog from which we randomly picked stellar hosts (with their corresponding properties) for each simulated planetary system. In the next subsections, we describe how we chose physical and orbital parameters for the planets in each system.

### 2.2. Planet Period and Radius Distribution

We assigned values for the period and radius of each simulated planet by drawing from debiased distributions. To create such debiased distributions, we started with the observed sample of *Kepler* candidate planets (or *Kepler* Objects of Interest; KOIs) and converted it to a debiased sample of planets using detection efficiencies. First we will discuss how we filtered the KOI catalog, and then we will discuss the calculation and application of detection efficiencies.

Our observed sample of KOIs is based on the 2012 February release (Q1–6) by Batalha et al. (2012) consisting of 2321 planetary candidates in 1790 systems. We only considered a subset of this KOI catalog by applying the following filters. First, we only considered planet candidates with positive values for their entries: we removed any planet candidates with negative values of the orbital period because such candidates are only based on a single transit (Batalha et al. 2012), and we also removed KOI 1611.02, the circumbinary planet also known as Kepler-16b (Doyle et al. 2011), because many of its entries in the catalog have negative values. This cut left us with 2298 remaining candidates. Next, we filtered out any planetary candidates with host stars that did not obey Equation (1) for consistency with the simulated stellar population. This step filtered out about half of the sample; 1135 candidates remained. Lastly, we made additional cuts based on planet radius, period, and signal-to-noise ratio (S/N):

$$\begin{aligned} P &\leq 200 \text{ days,} \\ 1.5 R_{\oplus} &\leq R \leq 30 R_{\oplus}, \\ S/N (\rightarrow Q8) &\geq 11.5. \end{aligned} \quad (2)$$

These specific cuts were performed in order to choose a sample of planetary candidates with period, radius, and S/N that are unlikely to be missed by the *Kepler* detection pipeline. It is necessary to choose a sample with a high degree of completeness because we want to compare this sample to simulations, which are normally 100% complete. For orbital periods, a range extending to 200 days ensures that multiple transits are likely to have been observed during Q1–6, which covers approximately 486.5 days. For planet radii, the lower bound on  $R$  of  $1.5 R_{\oplus}$  was chosen because the sample of observed planets with radii  $R \lesssim 1.5 R_{\oplus}$  has much lower detection efficiencies (e.g., Howard et al. 2012; Youdin 2011). For S/N, we required an  $S/N \geq 10$  for Q1–6, which corresponds to  $S/N \geq 11.5$  for Q1–8 by assuming that S/N roughly scales as  $\sqrt{N}$ , where  $N$  is the number of observed transits. This scaling is performed because the S/Ns of observed KOIs have been reported for Q1–8, not Q1–6, in Batalha et al. (2012). To investigate incompleteness issues, we have also repeated all analyses in this paper for S/N cuts of 15, 20, and 25.

Now we discuss how we calculated detection efficiencies, and how they were used to debias this filtered sample of planetary

<sup>3</sup> <http://archive.stsci.edu/pub/kepler/catalogs/>

candidates. Following the formalism of Youdin (2011), for any given planet the net detection efficiency  $\eta$  is the product of (1) the geometrical selection effect  $\eta_{\text{geom}}$  and (2) the *Kepler* photometric selection effect  $\eta_{\text{phot}}$ . The geometrical selection effect is due to the probability of transit as planets with longer periods or larger semimajor axes will have a lower probability of crossing in front of the disk of the star as seen from *Kepler*, and is calculated as  $\eta_{\text{geom}} = R_*/a$ , where  $a$  is semimajor axis. The *Kepler* photometric selection effect is due to the photometric quality of the star for detecting planets with specified radius and period. Consequently,  $\eta_{\text{phot}}$  is a function of both planetary radius and period. For a planet with radius  $R$  and period  $P$ , we calculated  $\eta_{\text{phot}}$  as the fraction of stars that can detect such a planet with  $S/N \geq 10$  (see Section 3.1), based on the KIC sample obtained in the previous section. Lastly, we calculated the net detection efficiency as  $\eta = \eta_{\text{geom}}\eta_{\text{phot}}$ .

We applied the above methods for obtaining detection efficiencies to our KOI subset of observed planetary candidates. For each candidate planet (or detection) in our KOI subset, we calculated its net efficiency  $\eta$  given its observed period  $P$  and radius  $R$ . Since  $\eta$  is the ratio of the number of detectable events to the number of actual planets, the inverse of  $\eta$  is equal to an estimate of the actual number of planets represented by each detection. After we calculated the value of  $1/\eta$  for each detection in our KOI subset, we created debiased, binned histograms for  $P$  and  $R$  representing an estimate of the actual number of planets per  $P$  or  $R$  bin. The normalized versions of these histograms are given in Figure 1. We used these discrete distributions representing debiased planet periods and radii in order to randomly select values for each simulated planet’s period and radius.

Our methods of obtaining photometric detection efficiencies ( $\eta_{\text{phot}}$ ) are the same as the methods described in Howard et al. (2012) used to obtain binned (in  $P$  and  $R$ ) efficiencies that were later analytically fit by Youdin (2011), except for the following differences. First, we applied these methods to Q1–6 data (previous work used Q2 only). Second, we avoided any loss of information that can occur during the binning process and/or the power-law fitting process by skipping those steps and directly calculating the detection efficiency for each individual KOI candidate in our filtered sample. Third, we calculated  $S/N$  differently by actually using each KIC star’s observing history during Q1–6 (e.g., not all stars are observed each quarter) as well as some other minor differences; our methods for calculating  $S/N$  are detailed in Section 3.1.

### 2.3. Planet Multiplicity Distribution

We chose to represent the multiplicity distribution of simulated planetary systems—the distribution of the number of planets per star—by either a delta-like distribution, a modified Poisson distribution, or a bounded uniform distribution. All distributions are described by a single parameter. We did not consider other distributions such as an exponential distribution, which may result in a bad fit to the data (Lissauer et al. 2011b). All stars in our model populations are assumed to have at least one planet, and so our study cannot directly address the question of planet occurrence.

A delta-like distribution is a discrete distribution described by a single parameter  $D$ . If the parameter  $D$  represents an integer value, then all planetary systems following this distribution will have  $D$  planets each. If the parameter  $D$  does not represent an integer value, then each planetary system can have either  $\lfloor D \rfloor$  (floor function) or  $\lceil D \rceil$  (ceiling function) planets. For instance, a model population with  $D = 3$  means that all of its planetary

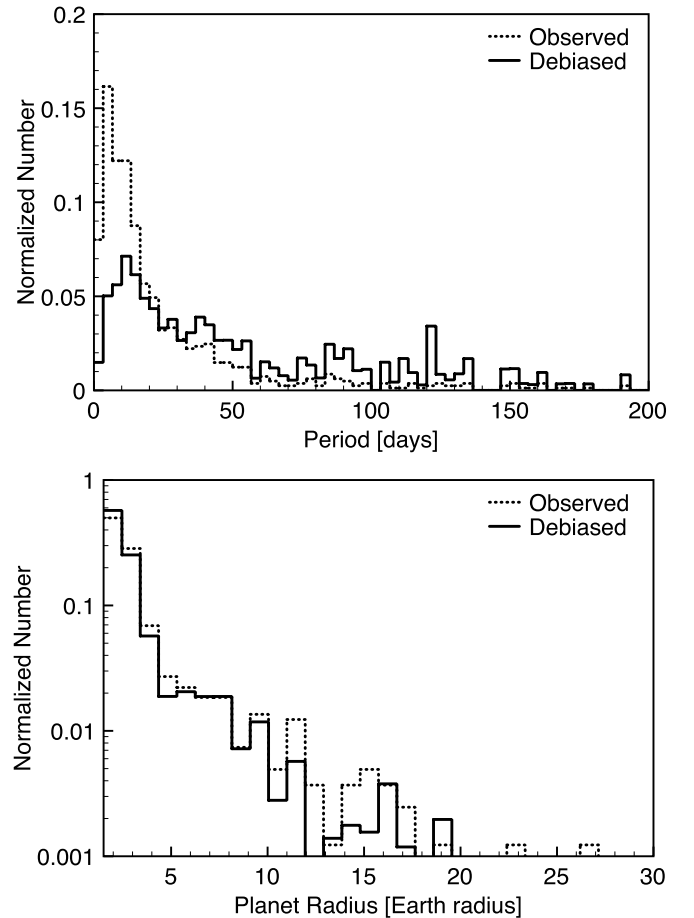


**Figure 1.** Observed and debiased distributions of orbital periods and radii for a subset (Equation (2)) of the planets detected by *Kepler*. The top plot for orbital period shows a distribution for 0–200 days divided into 60 equal-sized bins. The observed distribution shows increasing planet frequency at shorter periods, mainly due to the greater geometric probability of observing transiting planets at shorter periods. The bottom plot for planet radius shows a distribution for 1.5–30  $R_{\oplus}$  divided into 30 equal-sized bins.

systems have three planets per star, and a model population with  $D = 4.75$  means that 25% of its planetary systems have four planets and 75% of its planetary systems have five planets. As a result,  $D$  also represents the mean number of planets per system. This is the same as the “uniform” distribution used by Lissauer et al. (2011b).

A modified Poisson distribution described by parameter  $\lambda$  is a discrete distribution that is equivalent to a regular Poisson distribution with mean value  $\lambda$ , except that we ignore zero values. Therefore, by using a modified Poisson distribution we restrict the regular Poisson distribution so that values picked from the distribution must be greater than 0 (so that each planetary system must have at least one planet). As a result, the modified Poisson distribution is not strictly Poisson since its mean value is different from  $\lambda$ , hence the name “modified Poisson.” Mathematically, the regular Poisson distribution can be written as

$$P(k) = \frac{\lambda^k e^{-\lambda}}{k!}, \quad (3)$$

which gives the probability of obtaining a discrete value  $k$  from such a distribution.

A bounded uniform distribution is represented by a single parameter  $\lambda$ . For each planetary system, first a modified Poisson

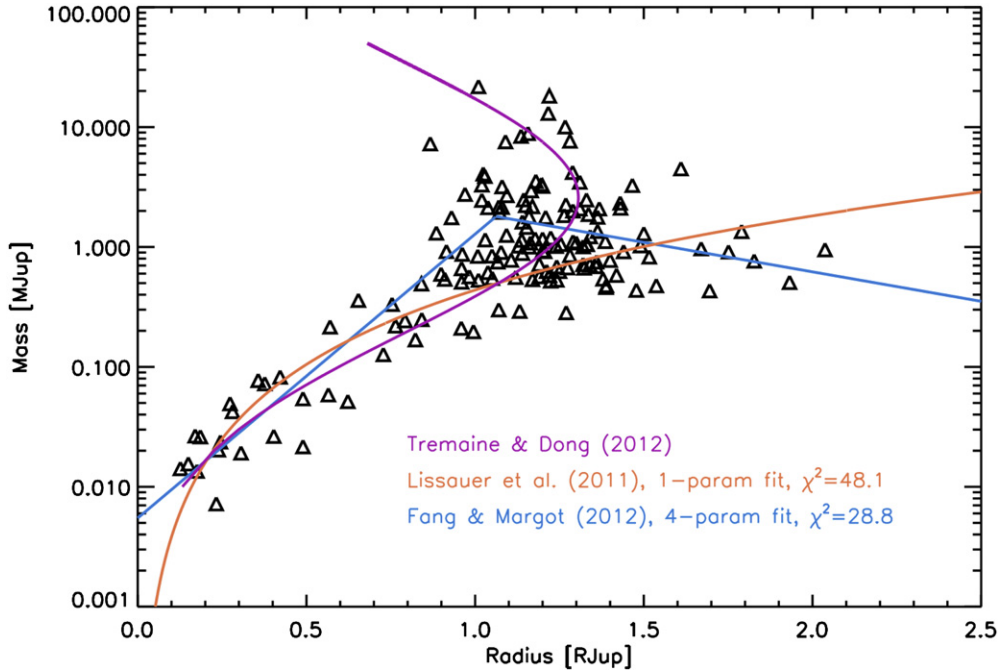


**Figure 2.** Known transiting planets (triangles) and three different mass–radius relations (colored curves). See Section 2.5 for details. (A color version of this figure is available in the online journal.)

distribution (as defined above) with parameter  $\lambda$  is used to draw a value  $N_{\max}$  (maximum number of planets). Second, a discrete uniform distribution with range  $1-N_{\max}$  is used to draw a value representing the number of planets in that system.

We varied the values of the parameter  $D$  for the delta-like distribution and the values of the parameter  $\lambda$  for the modified Poisson and bounded uniform distributions. In total, we explored  $D = 2-7$  and  $\lambda = 1-6$ , each with intervals of 0.25, resulting in a total of 63 possibilities for the multiplicity distribution.

#### 2.4. Planet Inclination Distribution

We chose the inclination distribution in each planetary system to be one of three possibilities: an aligned inclination distribution, a Rayleigh distribution, or a Rayleigh of Rayleigh distribution, as also used by Lissauer et al. (2011b).

An aligned distribution is the straightforward case where relative inclinations in the system are  $0^\circ$ . This is the same as a perfectly coplanar system.

A Rayleigh distribution is a continuous distribution described by a single parameter  $\sigma$ , which determines the mean and variance of the distribution. Its mathematical form is

$$P(k) = \frac{k}{\sigma^2} e^{-k^2/2\sigma^2}, \quad (4)$$

which gives the probability density function for a value  $k$  from this distribution.

A Rayleigh of Rayleigh distribution, with a single parameter  $\sigma_\sigma$ , means that we draw from two Rayleigh distributions for each planetary system. First, the given parameter  $\sigma_\sigma$  defines the first Rayleigh distribution from which we draw a value for  $\sigma$  for each planetary system. Second, the drawn value of  $\sigma$  is then used to define the second Rayleigh distribution from which we draw values for the inclinations of planets in that system. This allows for the possibility that planetary systems in a particular model population have Rayleigh inclination distributions with different mean and variance.

We varied  $\sigma$  for the Rayleigh distribution and  $\sigma_\sigma$  for the Rayleigh of Rayleigh distribution with the same range of values:  $1^\circ-10^\circ$  with intervals of  $1^\circ$ , as well as values of  $15^\circ$ ,  $20^\circ$ , and  $30^\circ$ . In total, all possibilities for the 3 inclination distributions added up to a total of 27 possible inclination distributions.

#### 2.5. Other Planetary Parameters

So far we have defined the distributions used in drawing the orbital periods, radii, multiplicity, and orbital inclinations of simulated planetary systems. Now we discuss all other relevant planetary parameters: planet mass, orbital semimajor axis, eccentricity, and longitude of the ascending node.

To determine planet mass  $M$ , we require an  $M(R)$  relation to convert from radius to mass. First, we used  $(M/M_\oplus) = (R/R_\oplus)^{2.06}$ , which is a commonly used power law derived by fitting to Earth and Saturn (Lissauer et al. 2011b). Results given in this paper are based on this relation. Second, we obtained an alternate  $M(R)$  relation by fitting to masses and radii of known transiting exoplanets. This  $M(R)$  relation is a broken log-linear fit given as

$$\log_{10} \left( \frac{M}{M_{\text{Jup}}} \right) = 2.368 \left( \frac{R}{R_{\text{Jup}}} \right) - 2.261 \quad \text{for } \left( \frac{R}{R_{\text{Jup}}} \right) < 1.062, \quad (5)$$

$$\log_{10} \left( \frac{M}{M_{\text{Jup}}} \right) = -0.492 \left( \frac{R}{R_{\text{Jup}}} \right) + 0.777 \quad \text{for } \left( \frac{R}{R_{\text{Jup}}} \right) \geq 1.062. \quad (6)$$

This fit is plotted in Figure 2, along with data of known transiting exoplanets, the  $(M/M_\oplus) = (R/R_\oplus)^{2.06}$  relation by Lissauer et al. (2011b), and an  $R(M)$  log-quadratic fit by Tremaine &

Dong (2012). Our four-parameter fit is a better match to the data than the one-parameter prescription of  $(M/M_{\oplus}) = (R/R_{\oplus})^{2.06}$  (improvement in  $\chi^2$  from 48.1 to 28.8), and this is not simply due to the addition of model parameters ( $F$ -test at 99.96% confidence level).

In contrast to the fit by Tremaine & Dong (2012), our fit is an  $M(R)$  function and not an  $R(M)$  function and hence is useful for cases that require assigning masses corresponding to particular radii (i.e., our fit does not have an ambiguity where some values of  $R$  have multiple corresponding values of  $M$ , which makes it impossible to select a unique mass for a given radius). In addition, our fit covers the full range of parameter space in radii; the fit by Tremaine & Dong (2012) has a maximum radius value of about 1.3 Jupiter radii. We have repeated the analysis described in this paper using our fitted  $M(R)$  relation in Equations (5) and (6), and we find essentially the same results as when we used  $(M/M_{\oplus}) = (R/R_{\oplus})^{2.06}$ .

Each planet's semimajor axis is determined using the orbital period and Kepler's Third Law. For eccentricity, we assumed that all planets have circular orbits. *Kepler* candidates do not show evidence for large eccentricities (Moorhead et al. 2011), but we note that even moderate eccentricities ( $<0.25$ ) could affect transit durations in a manner similar to that caused by differences in inclinations of up to a few degrees. For the longitude of the ascending node of each planet's orbit, we drew an angle from a uniform distribution with values between  $0^\circ$  and  $360^\circ$ .

Now we have described all relevant stellar and planetary parameters to build a fictitious planetary system. In the next subsection, we describe stability constraints placed on these systems.

### 2.6. Stability Requirements

The first stability constraint is Hill stability, and we describe our implementation using the following example. In the construction of each planetary system, we add a first planet with its parameters chosen according to the methods already described. If the system's assigned multiplicity is greater than one, we add a second planet. The second planet is accepted only if it is Hill stable with the first planet, which occurs when

$$\Delta = \frac{a_2 - a_1}{R_{H1,2}} \gtrsim 3.46, \quad (7)$$

where  $a$  is the semimajor axis and  $R_{H1,2}$  is the mutual Hill radius defined as

$$R_{H1,2} = \left( \frac{M_1 + M_2}{3M_*} \right)^{1/3} \frac{a_1 + a_2}{2}, \quad (8)$$

(e.g., Gladman 1993; Chambers et al. 1996). Here,  $M$  represents mass and subscripts 1 and 2 denote the inner and outer planets, respectively. If the second planet is not accepted because it violates Hill stability with the first planet, then the second planet has its radius and orbital period (or equivalently, mass and semimajor axis) re-drawn until Hill stability is satisfied. We require that all adjacent planet pairs satisfy this Hill stability requirement. The assumption that adjacent planet pairs should be Hill stable is reasonable; out of the 885 planet candidates located in multi-planet systems detected during Q1–6 of the *Kepler* mission, only two pairs of planets are found to be apparently unstable by Fabrycky et al. (2012) on the basis of numerical integrations using nominal mass–radius scalings and circular orbit assumptions.

Following the methods of Lissauer et al. (2011b), we imposed a second stability constraint that any adjacent planet trio (any three neighboring planets) must satisfy

$$\Delta_{\text{inner pair of trio}} + \Delta_{\text{outer pair of trio}} \gtrsim 18. \quad (9)$$

As described for the example above for Hill stability cases, if the constraint in Equation (9) is not satisfied, a planet's properties are re-drawn until this stability requirement is fulfilled.

For the creation of multi-planet systems, we added planets to each system one at a time, where successful addition of a planet occurred when it fulfilled both stability criteria described above. For systems with a large multiplicity, at times it was not possible to satisfy stability constraints given our period range and therefore we allowed a maximum of 1000 attempts per star before discarding it. Therefore, in rare cases, some model populations have a slightly lower number of planetary systems.

### 2.7. Summary

In summary we have described the steps taken to assemble various model populations, each consisting of about  $10^6$  planetary systems. Each of these model populations follows different combinations of (1) multiplicity and (2) inclination distributions. Taking all combinations of the values for the tunable parameters in these distributions, there are a total of 1701 possibilities. Our goal is to take these model populations, run them through synthetic observations, and see which planets are transiting and detectable. The properties of these detectable planets will then be compared to the actual observed *Kepler* planets to determine which model produces acceptable fits. This allows us to determine the nature of underlying multiplicities and inclinations. In the next section, we discuss how we evaluate these model populations.

## 3. EVALUATING MODEL POPULATIONS

We describe our methods for evaluating each model population: (1) determining detectable, transiting planets, and (2) comparing them to the observed *Kepler* planets using statistical tests.

### 3.1. Determining Detectable, Transiting Planets

For each model population, we determined which of the planets in each planetary system were *transiting*. From the group of transiting planets, we determined which transiting planets were *detectable* based on S/N requirements. The following paragraphs describe these methods.

For each planetary system, we evaluated whether any of the planets were transiting. First we picked a random line of sight (i.e., picking a random point on the celestial sphere) from the observer to the system, and the plane normal to this line-of-sight vector determines the plane of sky. We then computed the planet–star distance projected on the plane of sky (e.g., see Winn 2010). The minimum in that quantity is the *impact parameter*, which we normalized by the stellar radius. A planet transits when its impact parameter is less than 1.

We calculated the S/N of transit events in order to determine whether or not each transiting planet would have been detectable during Q1–6 of the *Kepler* mission. To do so, first we randomly picked a MJD (Modified Julian Date) between the first and last cadence mid-times of Q1–6 by using the dates provided in the *Kepler* Data Release Notes<sup>4</sup> (DRN) 14 and 16. We assumed

<sup>4</sup> The DRN are available for download from MAST at [http://archive.stsci.edu/kepler/data\\_release.html](http://archive.stsci.edu/kepler/data_release.html).

that the planet transited on this randomly picked date, and we explored backward and forward in time using the planet’s orbital period in order to determine the dates of all transits during Q1–6. Next, we eliminated any transits that occurred in the gaps between quarters; such gaps are necessary to roll the spacecraft 90° to keep its solar arrays illuminated. In addition, not all stars are observed each quarter, for instance, due to CCD module failure. As a result, we used the planet’s host star observing log that recorded all observed quarters (see Section 2.1), and eliminated any transits that occurred in quarters where the host star was not observed. Next, we eliminated a small fraction of remaining transits in a random fashion to account for a 95% duty cycle because of observing downtimes (e.g., breaks for data downlink). After accounting for these issues, all remaining  $N$  transits for this planet were then counted and used to calculate the detection S/N as

$$S/N = \left( \frac{R}{R_*} \right)^2 \frac{\sqrt{N}}{\sigma_{\text{CDPP}}}, \quad (10)$$

where the first fraction represents the depth of the transit and  $\sigma_{\text{CDPP}}$  represents an adimensional noise metric (quadratically interpolated to the transit duration length using the set of measured {3 hr, 6 hr, 12 hr} CDPP values) for the planet’s host star (see Section 2.1). If the S/N is at least the value of the S/N threshold for detection ( $S/N \geq 10$ ), then the transiting planet is labeled as detectable.

### 3.2. Comparing to Observations

Here, we describe how we evaluated each model population’s goodness of fit when compared to observations. All model populations are distinct from each other due to the different parameter values chosen for their underlying multiplicity and inclination distributions. To evaluate how well each model population matches the observations, we compared them using two observables: (1) observed multiplicity vector and (2) observed distribution of normalized, transit duration ratios. These observables were computed for both the simulated planets and the KOI candidates.

We discuss these two types of observables in greater detail. The multiplicity vector  $\mu$  represents the number of systems observed with  $j$  transiting planets, where  $j = 1, 2, 3, 4, 5, 6, 7+$ . In other words, the multiplicity vector describes how many systems are observed to have a single planet, how many systems are observed with two planets, etc. Systems with seven or more planets are placed in the same multiplicity category:  $j = 7+$ . The normalized, transit duration ratio  $\xi$  is defined as (e.g., Fabrycky et al. 2012)

$$\xi = \frac{T_{\text{dur},1}/P_1^{1/3}}{T_{\text{dur},2}/P_2^{1/3}}, \quad (11)$$

where the transit duration  $T_{\text{dur}}$  is normalized by the orbital period raised to the 1/3 power  $P^{1/3}$ . Subscripts 1 and 2 represent any pair of planets in the same system where 1 denotes the inner planet and 2 denotes the outer planet. A  $j$ -planet system has a total of  $j(j-1)/2$  pairs. We decided to fit to values of  $\xi$  because they contain information on mutual inclinations of observed multi-planet systems. For instance, coplanar systems tend to have values of  $\xi > 1$  because the inner planet’s impact parameter is smaller and hence its normalized transit duration is longer. Fabrycky et al. (2012) used the observed

*Kepler* distribution of  $\xi$  to determine that the observed mutual inclinations are low at 1°–2°3.

We calculated the  $(\mu, \xi)$  observables for the subset of KOIs previously obtained in Section 2.2. We also calculated the  $(\mu, \xi)$  observables for each model population by considering all detectable, transiting planets.

Our next step was to obtain a statistical measure of each model population’s goodness-of-fit to the observed population by calculating a test statistic and its corresponding probability. A larger probability indicates a better match to observations. To compare multiplicity vectors  $\mu$ , we performed  $\chi^2$  tests, which are appropriate for discrete data.  $\chi^2$  tests are valid when the  $\chi^2$  probability distribution is a good approximation to the distribution of the  $\chi^2$  statistic (Equation (12)). As shown by theoretical investigations, the approximation is usually good when there are at least five discrete categories and at least five values in each category for the model population’s  $\mu$  (e.g., Hoel 1984). These requirements may not always be satisfied in our case, and so we also perform a randomization method to calculate chi-square probabilities, as described below. To compare  $\xi$  distributions, we performed Kolmogorov–Smirnov (K-S) tests, which can be used for continuous data. K-S tests have no restrictions on sample sizes, and are also distribution-free and so therefore can be applied for any kind of underlying distribution of the comparison samples (e.g., Stuart & Ord 1991). These tests are described in more detail below.

The  $\chi^2$  test used for comparing multiplicity vectors uses a  $\chi^2$  statistic  $\chi^2$  computed as (e.g., Press et al. 1992)

$$\chi^2 = \sum_j \frac{(O_j - E_j)^2}{E_j}, \quad (12)$$

where  $O_j$  represents an observed quantity, in this case the number of observed planetary systems with  $j$  planets,  $E_j$  represents an expected or theoretical value, in this case the number of simulated planetary systems with  $j$  detectable planets, and  $j$  represents the index of the multiplicity vector (i.e., 1 for one-planet systems,  $N$  for  $N$ -planet systems, etc.) being summed over. Scaling was performed to adjust the model multiplicity vector such that  $\sum O_j = \sum E_j$ . Large values of  $\chi^2$  represent worse fits and larger deviations between  $O_j$  and  $E_j$  quantities, meaning it is not likely the  $O_j$  values are drawn from the population represented by the  $E_j$  values. For comparison between each model population’s expected values and observed values, we only considered  $j$  indices where  $E_j \neq 0$  (noting the appearance of  $E_j$  in the denominator of Equation (12)). Since we must ignore categories with  $E_j = 0$ , we note that there may be cases (i.e., for the delta-like multiplicity distribution) where a given model population with only one-planet and two-planet systems may yield a low  $\chi^2$  even though it is in fact *not* a good match to the data, e.g., because it does not predict any 3+ planet systems that are actually observed. Model populations based on delta-like multiplicity distributions do not provide a good match to the data (Section 4). Consequently, we will not consider them further and none of the  $\chi^2$  probabilities presented in this paper suffer from this issue.

We computed two  $\chi^2$  probabilities for each calculation of the statistic in Equation (12). First, the standard  $\chi^2$  probability is an incomplete gamma function that can be computed with knowledge of  $\chi^2$  and the number of degrees of freedom. For our case, the number of degrees of freedom is equal to the number of indices with  $E_j \neq 0$  subtracted by 1 (to account for the scaling constraint). This standard

probability function is a good approximation as long as the number of bins or the number of values in each bin is large. Given that some higher- $j$  categories in our multiplicity vector may have low numbers, we performed a second calculation of the  $\chi^2$  probability using a more robust randomization method (e.g., Good 2006). In this method, we determined how often we could pick a new distribution from the model distribution with  $\chi_{\text{new,model}}^2$  (comparing new and model distributions) that was worse than the  $\chi_{\text{obs,model}}^2$  (comparing observed and model distributions). In practice, we randomly picked 10,000 times per model population and the fraction of them that yielded  $\chi_{\text{new,model}}^2 > \chi_{\text{obs,model}}^2$  represented the  $\chi^2$  probability. We found that in most cases, there was reasonable agreement between the  $\chi^2$  probabilities from the standard function and from the randomization method. The  $\chi^2$  probabilities quoted later in this paper are those obtained from the randomization method.

For the K-S test used for comparing  $\xi$  distributions, we calculated the K-S statistic and the standard K-S probability (e.g., Press et al. 1992). The K-S statistic  $D$  is the maximum difference of the absolute value of two distributions given as cumulative distribution functions, or

$$D = \max |O_{N_1}(\xi) - E_{N_2}(\xi)|, \quad (13)$$

where  $O_{N_1}(\xi)$  represents the observed cumulative distribution function of  $\xi$  values,  $E_{N_2}(\xi)$  represents the expected or model cumulative distribution function, and  $N_1$  and  $N_2$  is the number of  $\xi$  values for the observed and expected distributions, respectively. The significance or probability of  $D$  represents the chance of obtaining a higher value of  $D$ , and can be calculated with knowledge of  $D$  and the number of points  $N_1$  and  $N_2$ . This test is valid even with an unequal number of points, i.e.,  $N_1 \neq N_2$ . We note that  $N_2$  can vary significantly between model populations and this can affect the reliability of the calculated probability, such as when comparing a probability obtained from one model population to the probability obtained from another model. This is most pertinent for cases with large differences in  $N_2$  (i.e., between model populations with small and large multiplicities), where a poor fit is harder to discern when there are fewer model values  $N_2$  to compare to observed values. This issue can manifest itself as outliers in our results for model populations with fewer number of planets per system. As we will show, we do not find any evidence of such outliers in our results.

In the next section, we describe our calculations of these probabilities to evaluate the match between each model population and the data.

#### 4. RESULTS

In this section, we present the results for the fit between each model population and the KOI subset that obeys Equations (1) and (2), and these results are illustrated in Figures 3–5. We do not show any results incorporating the delta-like multiplicity distribution because it does not provide a good match to the data. We will describe each of these figures in turn.

Figure 3 shows the probabilities resulting from the  $\chi^2$  test that compared the observed and model multiplicity vectors (number of one-planet systems, number of two-planet systems, etc.). Most models can be ruled out with  $3\sigma$  confidence, and these tend to be systems with many planets and low inclinations or systems with few planets and high inclinations. On the other hand, models that are consistent with the data include systems of few planets with low inclinations or systems of many planets

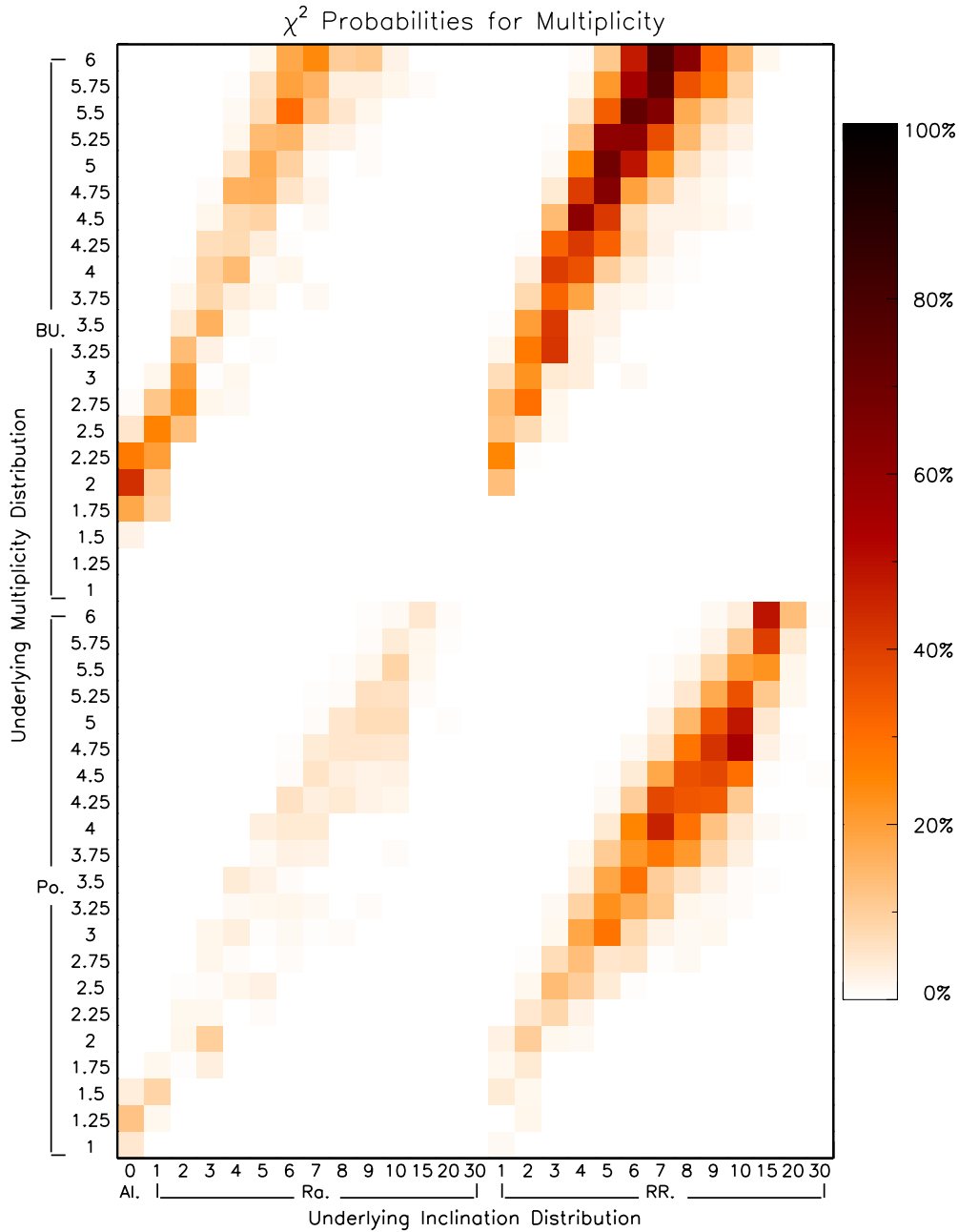
with high inclinations; this degeneracy is evident in the upward slopes in Figure 3. This degeneracy or upward trend is seen because the intrinsic populations corresponding to the observed transits can take a variety of forms: from few planets that are well aligned to many planets with larger inclinations. The degeneracy exists because systems with many planets and large inclinations are detected by transit surveys as systems with few planets and small inclinations. Models with a bounded uniform multiplicity distribution and a Rayleigh or Rayleigh of Rayleigh inclination distribution appear to provide a better fit (higher  $\chi^2$  probabilities) than other models.

Figure 4 depicts the probabilities from the K-S test that evaluated the fit between the observed and model  $\xi$  (Equation (11)) distributions of multi-planet systems. The distribution of  $\xi$  values is used to gauge the extent of coplanarity or non-coplanarity in multi-planet systems. This diagram shows that higher probabilities are obtained for models with low-inclination distributions. Nearly all models with a Rayleigh  $\sigma$  or Rayleigh of Rayleigh  $\sigma_\sigma$  parameter greater than  $3^\circ$  can be ruled out with  $3\sigma$  confidence. None of the models with perfectly aligned (coplanar) systems provide acceptable fits. The best fits with highest probabilities are Rayleigh or Rayleigh of Rayleigh inclination distributions with  $\sigma, \sigma_\sigma = 1^\circ$ . The probabilities in this figure appear to be relatively independent of the underlying multiplicity distribution (evident in the long vertical columns of blue colors), because the  $\xi$  distribution probes the relative inclination between any pair of planets in a system and is independent of the multiplicity or number of planets. As a result, we find that the K-S test is not very sensitive to the underlying multiplicity model. Comparison between Figures 3 and 4 shows that the degeneracy evident in Figure 3 is broken when considering Figure 4 as well—by also examining Figure 4, we see that only systems with fewer planets and lower inclinations are consistent with the data.

Figure 5 illustrates the combined probabilities from Figures 3 and 4. The combined probability is the product of the  $\chi^2$  and K-S probabilities. We make the assumption that these two probabilities are independent. This product of two probabilities is shown in Figure 5, from which it is evident that most models can be ruled out as unacceptable fits. Degeneracies present in both Figures 3 and 4 are broken when the data in these figures are combined in Figure 5. The best fits are models with lower inclinations and lower multiplicities, and in particular, the fits with a bounded uniform distribution in multiplicity and a Rayleigh or Rayleigh of Rayleigh distribution in inclination are most consistent with the data.

##### 4.1. Overall Best-fit Models: Few Planets and Low Inclinations

As seen in Figure 5, the overall best-fit models with the largest combined probabilities are models with low-multiplicity bound uniform distributions (represented by  $\lambda$ ) and with low-inclination Rayleigh (represented by  $\sigma$ ) or Rayleigh of Rayleigh (represented by  $\sigma_\sigma$ ) distributions. The best-fit model with a bounded uniform and Rayleigh distribution has  $\lambda = 2.50$  and  $\sigma = 1^\circ$ . The best-fit model with a bounded uniform and Rayleigh of Rayleigh distribution has  $\lambda = 2.25$  and  $\sigma_\sigma = 1^\circ$ . There are no qualitative differences between the quality of these two fits. Based on these two best-fit models, we find that 75%–80% of planetary systems have one or two planets with orbital periods less than 200 days. In addition, over 85% of planets have orbital inclinations less than  $3^\circ$  (relative to a common reference plane). These results represent our best estimate of the underlying distributions of *Kepler* transiting



**Figure 3.** Diagram showing probabilities from  $\chi^2$  tests that evaluated the goodness of fit of various models with respect to planet multiplicity. Each square on this grid represents a different model, and each square's color depicts the probability (the higher the probability, the better the fit). The  $x$ -axis shows the *underlying inclination distribution*, and can be aligned (Al.), Rayleigh (Ra.), or Rayleigh of Rayleigh (RR.). For Al., the number given is the inclination, or  $0^\circ$ . For Ra. and RR., the numbers indicate the  $\sigma$  or  $\sigma_\sigma$  parameter (in degrees) for the distribution. The  $y$ -axis shows the *underlying multiplicity distribution*, and can be modified Poisson (Po.) or bounded uniform (BU.). For Po, the number given is  $\lambda$  of the Poisson distribution and represents approximately the mean number of planets per system. For BU., the number given is  $\lambda$  of the Poisson distribution from which the maximum number of planets is drawn. This plot can be approximately divided into four quadrants, where in each quadrant the  $y$ -axis has the number of planets per system increasing to the top and the  $x$ -axis has inclinations increasing to the right.

(A color version of this figure is available in the online journal.)

systems for the parameter space explored here (Equations (1) and (2)). Assuming that the *Kepler* sample is representative, these distributions also describe the architecture of planetary systems in general.

We analyze the best-fit model with a bounded uniform ( $\lambda = 2.25$ ) and a Rayleigh of Rayleigh ( $\sigma_\sigma = 1^\circ$ ) distribution in greater detail. First, in Figure 6 we plot the underlying multiplicity and inclination distributions. The first and second rows of the figure show the first and second steps of picking

multiplicity and inclination values from the distributions. The plots in the bottom two rows show the resulting histograms of values picked from these distributions. Second, we show the comparisons between the best-fit model and the data. Table 1 compares the numbers of observed transiting systems to the numbers of detected transits from the best-fit model. There is a reasonable match in each multiplicity index and an overall match probability of 25.2%. Figure 7 illustrates the comparison between the distribution of  $\xi$  values from *Kepler* observations

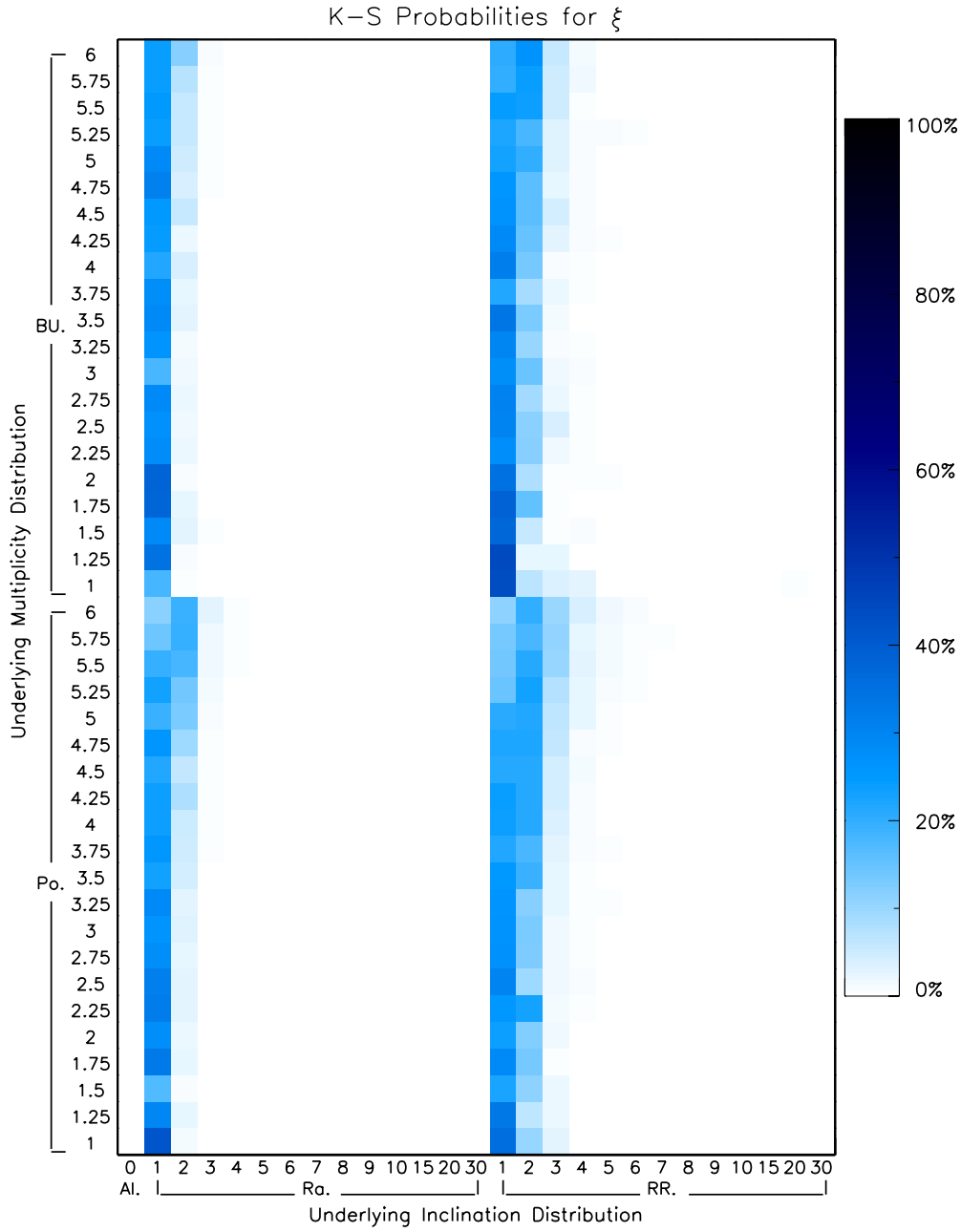


**Figure 4.** Same as Figure 3, except this diagram shows K-S probabilities of  $\xi$  distributions. These probabilities represent the goodness of fit of various models with respect to orbital inclinations.

(A color version of this figure is available in the online journal.)

**Table 1**

Multiplicity Vector: Number of Systems with  $j$  Detectable Planets

Name	$j =$	1	2	3	4	5	6	7+
Observed		542	85	24	4	1	1	0
Best-fit		540.6	92.9	19.1	3.6	0.6	0.2	0.0

**Note.** Comparison of the multiplicity vector between observations and one of two best-fit models, here with  $\lambda = 2.25$  and  $\sigma_\sigma = 1^\circ$  (see Section 4.1). The  $\chi^2$  probability for this match is 25.2%.

and the distribution of  $\xi$  values from simulated detections using the best-fit model. The numbers in each bin have been normalized to enable comparison, and the match between distributions has a probability of 27.5%. Taken together, the

probabilities from each fitted observable ( $\chi^2$  probability for the multiplicity fit and K-S probability for the  $\xi$  distribution fit) are multiplied to yield a combined probability of 6.9%.

The low inclinations in our best-fit models have interesting implications for planet formation and evolution theories. Our findings that these systems are relatively coplanar (at least out to 200 days) are in favor of standard models that suggest planet formation within a protoplanetary disk. In addition, strong influences by external perturbers such as Kozai processes, scattering, or resonances are not likely to play a major, lasting role given that these systems do not generally have high, excited inclinations. Theories of planet formation and evolution can be tested against the architecture of planetary systems illuminated by the *Kepler* mission.

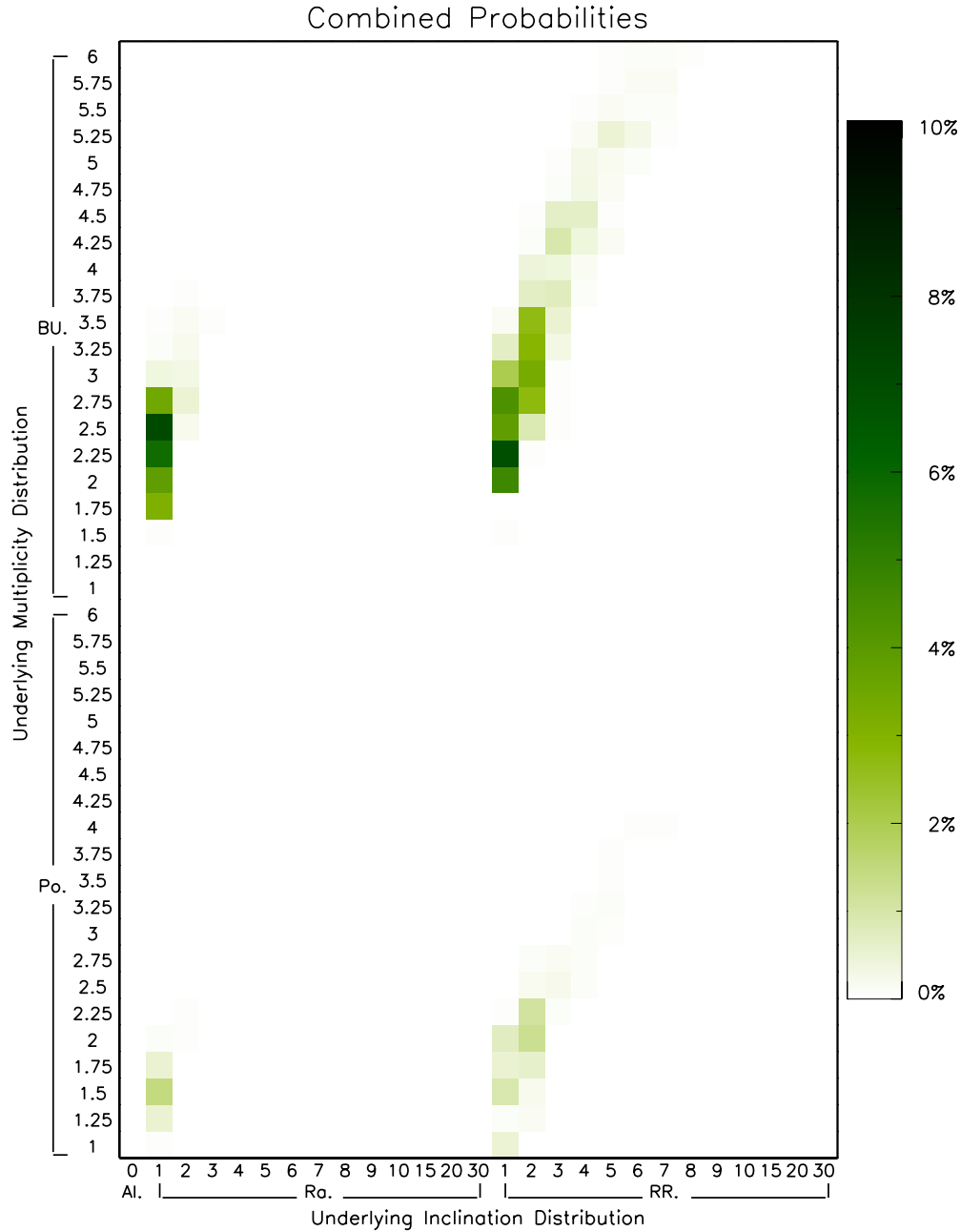


**Figure 5.** Same as Figure 3, except this diagram shows combined (multiplied) probabilities from  $\chi^2$  and K-S tests. These probabilities represent the overall goodness of fit of various models to the *Kepler* sample.

(A color version of this figure is available in the online journal.)

#### 4.2. Effects of False Positives and Search Incompleteness

The results of our study do not take into account the existence of false positives that mimic real planet transit signals in the *Kepler* data set. For the *Kepler* sample released by Borucki et al. (2011b), Morton & Johnson (2011) estimated that false positive probabilities were generally low at  $\lesssim 10\%$ , and an analysis using binary statistics by Lissauer et al. (2012) estimated that  $\sim 98\%$  of the multi-planet systems are real. For the latest *Kepler* sample released by Batalha et al. (2012), Fabrycky et al. (2012) discussed how  $\sim 96\%$  of pairs in multi-transiting candidate systems are likely to be real planets using stability arguments. For the purposes of our study, we assumed that all planetary candidates are real. We expect that the existence of false positives can potentially affect the fit between multiplicity

vectors (e.g., Table 1), particularly for the case of singly transiting systems where the actual population may actually have lower numbers than reported due to false positives. We do not expect that false positives will significantly influence the fit between normalized transit duration ratios (e.g., Figure 7) since such ratios are only computed for multi-planet systems, which we expect to be a higher-fidelity sample than singly transiting systems.

To determine the effect of false positives on our results, we repeated the entire analysis described in this paper for two cases. In the first case, we removed all false positives described in the literature (Howard et al. 2012; Batalha et al. 2012; Fabrycky et al. 2012; Santerne et al. 2012; Ofir & Dreizler 2012; Colón et al. 2012); a total of 35 false positives were removed from

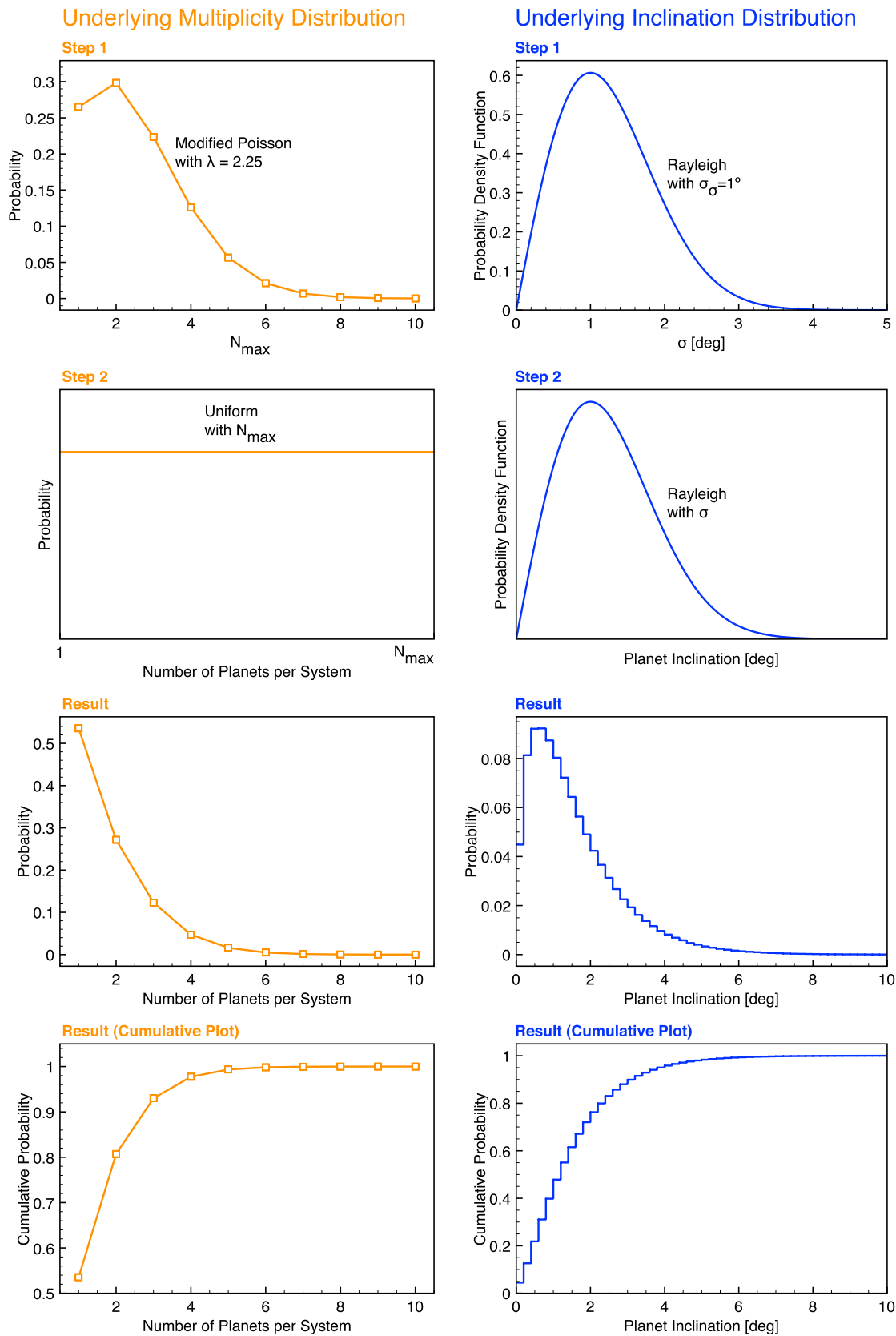


**Figure 6.** One of two best-fit models for multiplicity (left column) and inclination (right column). The multiplicity distribution is a bounded uniform distribution: for each planetary system (1) we draw a value  $N_{\max}$  from a modified Poisson distribution with  $\lambda = 2.25$ , and (2) we choose the number of planets by uniformly picking a value between 1 and  $N_{\max}$ . The resulting distributions of multiplicities are shown in the bottom plots. The inclination distribution is a Rayleigh of Rayleigh distribution: (1) for each planetary system we draw a value for  $\sigma$  from a Rayleigh distribution with parameter  $\sigma_\sigma = 1^\circ$ , and (2) for each of its planets we draw a value for inclination from a Rayleigh distribution with parameter  $\sigma$ . The resulting distributions of inclinations are shown in the bottom plots.

(A color version of this figure is available in the online journal.)

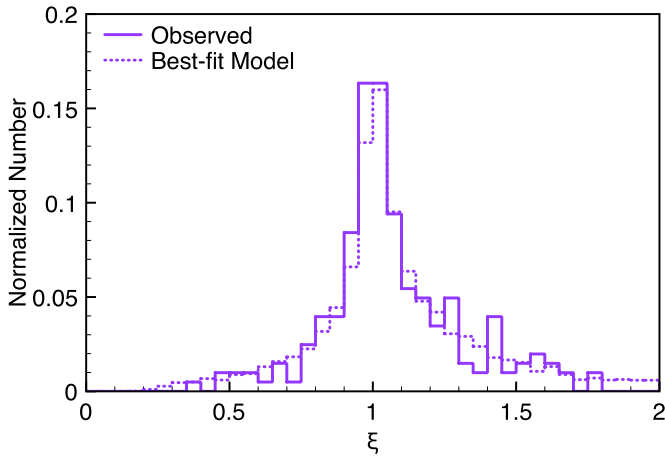


**Figure 7.** Comparison of the  $\xi$  distribution between observations and one of two best-fit models, here with  $\lambda = 2.25$  and  $\sigma_\sigma = 1^\circ$  (Section 4.1). The quantity  $\xi$  is sensitive to orbital inclinations in multi-planet transiting systems. The K-S probability for this match is 27.5%.

(A color version of this figure is available in the online journal.)

the KOI table. Since we base our debiased period and radius distributions on the observed sample, we created new model populations and repeated our analyses. In the second case, not only did we remove all known false positives but we also added simulated false positives to our artificial populations. For each population of planetary systems, we added enough false positives (all single-planet systems) such that false positives represented 10% of all planets. The properties of the simulated false positives (e.g., radius and period) were based on the properties of known false positives. We then repeated all of our analyses for these populations. In both cases, we found that our results of intrinsic distributions were almost identical in terms of the typical number of planets per system as well as their inclinations. Accordingly, we do not expect that the effect of false positives will appreciably change our results.

Another effect that can impact our results is *Kepler* search incompleteness. The *Kepler* team is currently investigating the completeness of the pipeline by inserting artificial transits into the pipeline and determining their recovery rates. Batalha et al. (2012) suggested that the KOI catalog released in 2011 by Borucki et al. (2011b) suffers from incompleteness issues because the planet gains seen between the 2011 and 2012 catalogs cannot be completely explained by the longer observation window, and that it is possible the 2012 catalog still suffers from some incompleteness issues. This can affect our results in terms of the comparison between the observations and our model’s computed observables, and we expect that its impact is a function of S/N and other parameters. The impact of incompleteness will be better known after the *Kepler* team’s detailed study of pipeline completeness is finished, and pipeline completeness is expected to improve in the future with pipeline upgrades that are already underway (Batalha et al. 2012).

To investigate the reliability of our results given incompleteness issues, we have repeated all simulations and analyses described in this paper for higher S/N thresholds of 15, 20, and 25. In all cases, we find that our conclusions regarding low intrinsic inclinations are the same and that the *Kepler* data favor low-inclination distributions. However, we find that the best-fit multiplicity distribution rises toward larger numbers of planets as we increase to higher S/N thresholds. This can be explained as follows. For a given population of planetary systems, by

imposing higher and higher S/N thresholds on the detectability of its transiting planets, planets in two-planet systems are more likely to be missed than planets in one-planet systems. This is because the outer planet in two-planet systems tends to have a larger orbital period than the planet in one-planet systems, and therefore the outer planet in two-planet systems will exhibit fewer transits and have lower S/N. Consequently, the ratio of observed one-planet to two-planet systems should rise with higher S/N thresholds for detectability. This effect is seen in our synthetic populations, but is not seen in the observed *Kepler* data, where the ratio of observed one-planet to two-planet systems remains near 6:1 for S/N  $\sim 10$  to S/N  $\sim 25$  for the radius and period regime considered here. As a result, the best-fit multiplicity distribution rises with increasing S/N thresholds in order to match the data. This curious trend in the data suggests that perhaps there are many single-planet systems missing in the KOI table. If this is the case, then our multiplicity determinations serve as an upper limit regarding the typical number of planets per system. The best way to test this is to repeat this analysis in the future when the KOI tables are less biased and more complete.

## 5. COMPARISON WITH THE SOLAR SYSTEM AND WITH PREVIOUS WORK

We compare the results of our study with the properties of planets in the solar system as well as with some relevant previous studies.

### 5.1. Results are Consistent with the Solar System

Based on the underlying multiplicity distribution of our best-fit models, 75%–80% of planetary systems have one or two planets with orbital periods less than 200 days (see Section 4.1). In comparison, the solar system has one planet, Mercury, with an orbital period less than 200 days. Accordingly, our best-fit multiplicity distributions are consistent with the solar system, if we extrapolate the results of our study to planetary radii less than 1.5 Earth radii. Note that our analysis is agnostic about the number of planets with larger orbital periods or different radius/mass regimes than considered here; recall that these limits are due to the parameter space constraints imposed by our study and defined in Equations (1) and (2). More data and extension of this study to longer orbital periods and smaller planetary radii are warranted before any definitive multiplicity comparison can be made with the solar system.

Based on the underlying inclination distributions of our best-fit models, over 85% of planets have orbital inclinations less than  $3^\circ$  (see Section 4.1), suggesting a high degree of coplanarity. This is compatible with the inclinations seen among the planets in the solar system, if we allow ourselves to extrapolate beyond the period and radii limits of our study. In the solar system, seven out of the eight planets (or 87.5%) have inclinations less than  $3^\circ$  relative to the invariable plane, with Mercury as the exception.

### 5.2. Comparison with Previous Studies

Lissauer et al. (2011b) investigated the dynamical properties of multi-planet systems in the KOI catalog announced by Borucki et al. (2011b). They also presented a detailed analysis of the inclinations of *Kepler* planetary systems. To accomplish this, they created a host of planetary models following different planet multiplicity and inclination distributions, determined which of those planets were transiting and detectable, and compared the resulting transit numbers with the observed transit

numbers to determine each model’s goodness of fit. Differences between their methods and ours include different methods for obtaining debiased period and radius distributions, different radius and period parameter ranges, an observed  $\xi$  distribution that was used as a fitted observable in our study, and different data sets (we used the most recently released KOI data set; Batalha et al. 2012). From their results, Lissauer et al. (2011b) ruled out systems with small numbers of planets and large inclinations as well as systems with large numbers of planets and small inclinations, which we also found to be inconsistent with the data (see Figure 3). In addition, they found a degeneracy in their results between underlying distributions of inclination and multiplicity; the number of planets per system could be increased if the inclination was also increased and still provide good fits to the data, also seen in our Figure 3. Ultimately, they discounted the case of thick systems with many planets by invoking results from radial velocity surveys that suggested low inclinations (see discussion in Fabrycky et al. 2012). In our study, we were able to reject that scenario because it provided poor fits to the observed  $\xi$  distribution (see Figure 4).

Tremaine & Dong (2012) applied a general statistical model to *Kepler* data as well as to radial velocity surveys to analyze the multiplicity and inclination distributions. They concluded that *Kepler* data alone could not place constraints on inclinations, and acceptable possibilities ranged from thin to even spherical systems. Systems with large rms inclinations could be fit by the data as long as some of them had a large number of planets. However, when jointly analyzing both *Kepler* and radial velocity data, they were able to place constraints on inclinations to show that mean planetary inclinations are in the range  $0^\circ$ – $5^\circ$ . These relatively low inclinations are consistent with our results showing how models with lower inclinations provided better fits to the data.

Figueira et al. (2012) determined underlying inclination distributions by applying information from both High Accuracy Radial Velocity Planet Searcher (HARPS) and *Kepler* surveys. They assumed that if the HARPS and *Kepler* surveys share the same underlying population, then the different detection sensitivities of these two surveys with their detected samples of planets should allow determination of the underlying inclinations. To do so, they created synthetic populations of planets with a given multiplicity distribution as previously determined using HARPS data, and planets were given various inclination distributions (aligned, Rayleigh, and isotropic). Each model’s goodness of fit was determined by comparing the frequency of transiting systems with the *Kepler* sample. They found that the best fits were obtained using models with inclinations prescribed by a Rayleigh distribution with  $\sigma \leq 1^\circ$ . In our study, we used a different data set based on the latest release by Batalha et al. (2012), we fit for an additional parameter (the intrinsic multiplicity distribution), and we fit to an extra observable (the resulting  $\xi$  distribution). Given that, our overall results are in agreement since we also found that low inclinations with a Rayleigh parameter  $\sigma \sim 1^\circ$  are consistent with the data.

Fabrycky et al. (2012) presented important properties of multi-planet candidates in the KOI catalog released by Batalha et al. (2012). They found that almost all of these systems are apparently stable (using nominal mass–radius and circular orbit assumptions), which reinforces the high-fidelity nature of these multi-planet detections. In addition, they derived the mutual inclinations of observed planets using the distribution of  $\xi$  from the *Kepler* sample, which we used in our study as a fitted observable. They found that mutual inclinations are constrained

to the range of  $1^\circ$ – $2.3^\circ$  for observed planets, and concluded that planetary systems are typically flat. Our analysis is different and has some advantages in that we considered underlying planet multiplicity and inclination models, ran them through synthetic observations, and fitted the models’ results to observed transit numbers and  $\xi$  distribution. Our study agrees with the conclusions of Fabrycky et al. (2012) that planetary systems tend to be relatively coplanar to within a few degrees.

Weissbein et al. (2012) implemented an analytical model and investigated an intrinsic Poisson distribution for planet multiplicity as well as coplanar and non-coplanar assumptions for inclinations using a Rayleigh distribution. They found that none of their choices for multiplicity and inclination distributions produced numbers of transiting planet systems matching the *Kepler* data. This is generally consistent with our results, where we find that combinations of Poisson multiplicity distributions and Rayleigh inclination distributions produce some of the poorest fits. They suggested that the disagreement between their results and the data could be potentially explained if planet occurrence is not an independent process and is instead correlated between planets in the same system, where the existence of one planet may affect the existence of additional planets.

Johansen et al. (2012) used a different approach than some previous authors. They created synthetic triple planet systems by assuming they could be based off of observed *Kepler* triply transiting systems. They determined which of their synthetic planets could be transiting and observable, and then calculated the resulting number of singly, doubly, and triply transiting systems to compare with the actual number of transits in the *Kepler* data. They also repeated these steps for different inclinations. From fitting to observed doubly and triply transiting systems, they found low mutual inclinations of  $\lesssim 5^\circ$ . Although our methods are different, such low mutual inclinations are compatible with our findings that these systems are intrinsically thin. In addition, Johansen et al. (2012) found that numbers of transiting two-planet and three-planet systems can be matched by underlying three-planet systems, but they underproduced the number of transiting single-planet systems. To investigate this further, we have repeated our entire analysis by considering systems with only one or three planets. We find that we are not only able to reproduce the numbers of transiting two-planet and three-planet systems, as did Johansen et al. (2012), but also the number of single planet systems. Of course, by considering only systems with one and three planets we are not able to match the number of systems with four transiting planets or greater.

## 6. CONCLUSIONS

We have investigated the underlying distributions of multiplicity and inclination of planetary systems by using the sample of planet candidates discovered by the *Kepler* mission during Quarters 1–6. Our study included solar-like stars and planets with orbital periods less than 200 days and with radii of  $1.5$ – $30 R_\oplus$ . We created model populations represented by a total of two tunable parameters, and we fitted these models to observed numbers of transiting systems and to normalized transit duration ratios. We did not include any constraints from radial velocity surveys. Below we list the main conclusions of our study.

1. From our best-fit models, 75%–80% of planetary systems have 1 or 2 planets with orbital periods less than 200 days. This represents the unbiased, underlying number of planets per system.

2. From our best-fit models, over 85% of planets have orbital inclinations less than  $3^\circ$  (relative to a common reference plane), implying a high degree of coplanarity.
3. Compared to previous work, our results do not suffer from degeneracies between multiplicity and inclination. We break the degeneracy by jointly considering two types of observables that contain information on both number of planets and inclinations.
4. If we extrapolate down to planet radii less than 1.5 Earth radii, the underlying multiplicity distribution is consistent with the number of planets in the solar system with orbital periods less than 200 days. If we also extrapolate to beyond 200 days, we find that the underlying distribution of inclinations derived here is compatible with inclinations in the solar system.
5. Our results are also consistent with the standard model of planet formation in a disk, followed by an evolution that did not have a significant and lasting impact on orbital inclinations.

Continued observations by the *Kepler* mission will improve the detectability of new candidate planets covering a larger swath of parameter space, especially to longer orbital periods and smaller planetary radii. We anticipate that future statistical work will further boost our understanding of the underlying architecture of planetary systems.

We thank Dan Fabrycky for useful discussions, as well as the entire *Kepler* team for procuring such an excellent data set of planetary systems. We also thank the reviewer for helpful comments that improved the paper.

## REFERENCES

- Baluev, R. V. 2011, *Celest. Mech. Dyn. Astron.*, **111**, 235
- Batalha, N. M., Borucki, W. J., Bryson, S. T., et al. 2011, *ApJ*, **729**, 27
- Batalha, N. M., Rowe, J. F., Bryson, S. T., et al. 2012, arXiv:1202.5852
- Bean, J. L., & Seifahrt, A. 2009, *A&A*, **496**, 249
- Borucki, W. J., Koch, D. G., Basri, G., et al. 2011a, *ApJ*, **728**, 117
- Borucki, W. J., Koch, D. G., Basri, G., et al. 2011b, *ApJ*, **736**, 19
- Brown, T. M., Latham, D. W., Everett, M. E., & Esquerdo, G. A. 2011, *AJ*, **142**, 112
- Chambers, J. E., Wetherill, G. W., & Boss, A. P. 1996, *Icarus*, **119**, 261
- Christiansen, J. L., Jenkins, J. M., Barclay, T. S., et al. 2012, arXiv:1208.0595
- Colón, K. D., Ford, E. B., & Morehead, R. C. 2012, arXiv:1207.2481
- Correia, A. C. M., Couetdic, J., Laskar, J., et al. 2010, *A&A*, **511**, A21
- Doyle, L. R., Carter, J. A., Fabrycky, D. C., et al. 2011, *Science*, **333**, 1602
- Fabrycky, D. C., Lissauer, J. J., Ragozzine, D., et al. 2012, arXiv:1202.6328
- Figueira, P., Marmier, M., Boué, G., et al. 2012, *A&A*, **541**, A139
- Fressin, F., Torres, G., Désert, J.-M., et al. 2011, *ApJS*, **197**, 5
- Gladman, B. 1993, *Icarus*, **106**, 247
- Good, P. I. 2006, *Resampling Methods: A Practical Guide to Data Analysis* (3rd ed.; Boston, MA: Birkhauser), 218
- Hoel, P. 1984, in *Introduction to Mathematical Statistics*, Wiley Series in Probability and Mathematical Statistics. Probability and Mathematical Statistics, (New York: Wiley)
- Holman, M. J., Fabrycky, D. C., Ragozzine, D., et al. 2010, *Science*, **330**, 51
- Howard, A. W., Marcy, G. W., Bryson, S. T., et al. 2012, *ApJS*, **201**, 15
- Johansen, A., Davies, M., Church, R. P., & Holmélín, V. 2012, *ApJ*, **758**, 39
- Konacki, M., & Wolszczan, A. 2003, *ApJ*, **591**, L147
- Lissauer, J. J., Fabrycky, D. C., Ford, E. B., et al. 2011a, *Nature*, **470**, 53
- Lissauer, J. J., Marcy, G. W., Rowe, J. F., et al. 2012, *ApJ*, **750**, 112
- Lissauer, J. J., Ragozzine, D., Fabrycky, D. C., et al. 2011b, *ApJS*, **197**, 8
- McArthur, B. E., Benedict, G. F., Barnes, R., et al. 2010, *ApJ*, **715**, 1203
- Moorhead, A. V., Ford, E. B., Morehead, R. C., et al. 2011, *ApJS*, **197**, 1
- Morton, T. D., & Johnson, J. A. 2011, *ApJ*, **738**, 170
- Ofir, A., & Dreizler, S. 2012, arXiv:1206.5347
- Press, W. H., Teukolsky, S. A., Vetterling, W. T., & Flannery, B. P. 1992, *Numerical Recipes in FORTRAN. The Art of Scientific Computing* (Cambridge: Cambridge Univ. Press)
- Sanchis-Ojeda, R., Fabrycky, D. C., Winn, J. N., et al. 2012, *Nature*, **487**, 449
- Santerne, A., Díaz, R. F., Moutou, C., et al. 2012, *A&A*, **545**, A76
- Stuart, A., & Ord, J. 1991, *Kendall's Advanced Theory of Statistics, Vol. 2. Classical Inference and Relationship*, Kendall's Advanced Theory of Statistics (5th ed.; Oxford: Oxford Univ. Press)
- Tremaine, S., & Dong, S. 2012, *AJ*, **143**, 94
- Weissbein, A., Steinberg, E., & Sari, R. 2012, arXiv:1203.6072
- Winn, J. N. 2010, in *Exoplanets*, ed. S. Seager (Tucson, AZ: Univ. Arizona Press)
- Youdin, A. N. 2011, *ApJ*, **742**, 38